A comparison of theory and experiments on the dynamic plastic behavior of shells

N. JONES and R. M. WALTERS (CAMBRIDGE, MASS.)

A COMPARISON is made between the predictions of an approximate theoretical rigid-plastic procedure and some experimental values of the permanent deflections of hemispherical shells and cylindrical shell panels loaded impulsively. The initial kinetic energy of the dynamic loads in these tests was considerably larger than the maximum amount of strain energy which the shells could absorb in a wholly elastic manner. It emerged that reasonable agreement was obtained for the strain rate insensitive shells examined here and in Ref. [3] which should provide encouragement for the further development of these approximate procedures.

W pracy dokonano porównania między wynikami pewnego przybliżonego podejścia teoretycznego, opartego na modelu sztywno-plastycznym, a danymi doświadczalnymi dotyczącymi trwałych ugięć powłok półkulistych oraz odcinkowych powłok walcowych obciążonych w sposób nagły. Początkowa energia kinetyczna obciążeń dynamicznych, stosowanych w tych doświadczeniach, przewyższała znacznie maksymalną wartość energii odkształcenia, jaką powłoki były w stanie pochłonąć w sposób całkowicie sprężysty. Okazuje się, że uzyskano zadowalającą zgodność w przypadku rozważanych w pracy powłok niewrażliwych na prędkość odkształcenia z wynikami pracy [3]. Fakt ten powinien stanowić zachętę do dalszego rozwijania przedstawionej w pracy metody przybliżonej.

В работе даётся сравнение между результатами некоторого приближённого теоретического подхода, основанного на жёстко-пластической модели, и данными опытов по определению остаточных прогибов во внезапно нагружаемых полусферических или сегментных цилиндрических оболочках. Начальная кинетическая энергия динамического нагружения, производимого в этих опытах, значительно превышала величину энергии деформирования, которую оболочки способны поглотить в чисто упругом состоянии. Для исследуемых оболочек из материалов, нечувствительных к скоростям деформирования, получено удовлетворительное совпадение с результатами работы [3]. Этот факт должен поощрить дальнейшее развитие приближённого метода, предложенного в данной работе.

1. Introduction

AN EXPERIMENTAL investigation into the dynamic inelastic behavior of cylindrical shell panels and hemispherical shells has been reported recently in Refs. [1] and [2]. The initial kinetic energies of the dynamic loads in these tests were much larger than the maximum strain energies which the shells could absorb in a wholly elastic manner. It appears from these experimental results that the influence of material elasticity and finite-deflections or geometry changes does not exhibit a significant effect on the overall structural response at least for transverse deflections up to twice the corresponding shell thickness. Therefore, a rigid-plastic theoretical procedure, which is developed for infinitesimal deflections, should provide reasonable engineering estimates of the behavior of the strain rate insensitive cylindrical shell panels and hemispherical shells studied in Refs. [1] and [2].

An approximate theoretical procedure was developed in Ref. [3] in order to examine the dynamic behavior of arbitrarily shaped shells made from a rigid perfectly plastic ma-

terial. This method incorporated similar simplifications to those in the earlier analyses of SAWCZUK [4] and Ref. [5] on the respective static and dynamic behavior of initially flat plates. It was observed that the theoretical predictions [3] for the behavior of a complete spherical shell subjected to a spherically symmetric pressure puls and a fully clamped cylindrical shell loaded impulsively agreed favorably with more exact rigid plastic analyses.

In this article, the general procedure which is presented in Ref. [3] is used to study the dynamic inelastic behavior of hemispherical shells and cylindrical shell panels. These theoretical predictions are compared with the corresponding experimental results reported in Refs. [1] and [2].

2. Fully clamped spherical shell

The behavior of a deep spherical shell cap (Fig. 1), which is subjected to a uniformly distributed impulsive velocity V_0 which acts on the inner surface, will be examined using the approximate procedure outlined in Ref. [3].

It is assumed that the velocity field which characterizes the dynamic response of this problem is

$$(2.1)_{1,2} \qquad \dot{w}_0(\phi, t) = \frac{\dot{w}_0(t)(\cos\phi - \cos\phi_0)}{(1 - \cos\phi_0)}, \quad \text{and} \quad \dot{u}(\phi, t) = 0,$$
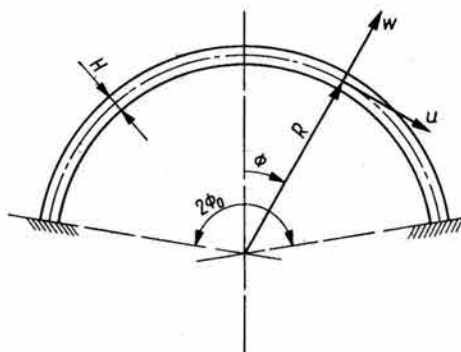

FIG. 1. Fully clamped spherical shell.

where $\dot{w}_0(t)$ is the transverse velocity at $\phi = 0$. Equations (2.1) are the same as those employed by ONAT and PRAGER [6] to obtain the static collapse pressure of a fully clamped spherical shell cap.

In order to satisfy the normality requirements of plasticity associated with the Tresca yield criterion, ONAT and PRAGER [6] showed that the velocity field (2.1) demands a membrane state of stress throughout most of the spherical shell except in a small region $\phi^* \leqslant$ $\leqslant \phi \leqslant \phi_0$ near the supports where

$$(2.2) \qquad \cos\phi^* = \frac{2\cos\phi_0}{2 - H/R}.$$

If σ_0 is the tensile yield stress, $N_0 = \sigma_0 H$ and $M_0 = \sigma_0 H^2/4$, then

(2.3) $$N_\theta = N_\phi = N_0 \quad \text{and} \quad M_\theta = M_\phi = 0$$

in the region $0 \leqslant \phi \leqslant \phi^*$ while

(2.4)$_1$ $$N_\theta = N_\phi = \frac{2R}{H} N_0 \frac{(\cos\phi - \cos\phi_0)}{\cos\phi}$$

and

(2.4)$_2$ $$M_\theta = M_\phi = M_0 \left\{ 1 - \frac{4R^2}{H^2} \frac{(\cos\phi - \cos\phi_0)^2}{\cos^2\phi} \right\}$$

in the outer zone $\phi^* \leqslant \phi \leqslant \phi_0$.

MARTIN and SYMONDS [7] showed for a rigid perfectly plastic structure, which is loaded impulsively, that the best agreement between a mode approximation [time-independent velocity field, for example, (2.1)] and the actual response, occurs when the initial character-istic mode velocity is ν times the exact impulsive velocity, where

(2.5) $$\nu = \frac{\int\limits_s \mu \dot{u}_i^* V_i \, ds}{\int\limits_s \mu \dot{u}_i^* \dot{u}_i^* \, ds}, \quad i = 1, 2, 3.$$

In Eq. (2.5), s is the surface area, μ the mass per unit area, $\dot{u}_i^*$ is a mode approximation of the initial velocity field and V_i is the actual impulsive velocity field which is determined from the applied impulse by momentum conservation. It is straightforward to show when substituting (2.1) into (2.5) that

(2.6) $$\nu \dot{w}_0 = 1.5 V_0,$$

where V_0 is an impulsive transverse velocity distributed uniformly over the entire middle surface of the spherical shell cap illustrated in Fig. 1.

The problem at hand involves the axisymmetric dynamic response of a shell of re-volution for which the influence of finite-deflections is not significant according to the observations in Ref. [2]. Thus, Eq. (15) in Ref. [3] becomes

(2.7) $$\int (p - \mu\ddot{w}) R^2 \sin\phi \, \bar{w} d\phi = \int (N_\phi + N_\theta) R \sin\phi \, \bar{w} d\phi - \int M_\theta \cos\phi \, \bar{w}' d\phi$$
$$- \sum_k \int M_\phi \sin\phi \, \bar{w}'' d\phi - \sum_l \{M_\phi \sin\phi\}_l [\bar{w}']_l,$$

which may be rewritten with the aid of Eqs. (2.1)–(2.4) as

(2.8) $$a_5 p - a_6 \ddot{w}_0 = a_7 p_c,$$

where

$$a_1 = 1/2(1 - \cos^2\phi^*) + \cos\phi_0 \cos\phi^* - \cos\phi_0,$$

$$a_2 = \frac{R}{H}\left[1/2(3\cos^2\phi_0 + \cos^2\phi^*) - 2\cos\phi_0\cos\phi^* + \cos^2\phi_0 \log\left(\frac{\cos\phi^*}{\cos\phi_0}\right)\right],$$

(2.9)$_{1-8}$ $$a_3 = \frac{H}{8R}\left[1/2(\cos^2\phi^* - \cos\phi_0) - \frac{4Ra_2}{H}\right],$$

$(2.9)_{1-8}$
[cont.]

$$a_4 = \frac{H\sin^2\phi_0}{8R},$$

$$a_5 = 1/2(1-\cos\phi_0)^2,$$

$$a_6 = 2/3\mu a_5,$$

$$a_7 = a_1+2a_2+2a_3+a_4 \quad \text{and} \quad p_c = \frac{2\sigma_0 H}{R}.$$

It should be noted in passing that $2\pi R^2 \dot{w}_0/(1-\cos\phi_0)$ times the right-hand side of Eq. (2.8) is the internal energy dissipation D, while $2\pi R^2 \dot{w}_0/(1-\cos\phi_0)$ times the left hand side of Eq. (2.8) is the external work rate.

It may be shown when satisfying the initial conditions $w_0 = 0$ and $\dot{w}_0 = \nu V_0$ that Eq. (2.8) gives

$$(2.10) \qquad\qquad w_0(t) = \frac{-a_7 p_c t^2}{2a_6} + \nu V_0 t.$$

The duration of motion t_f is obtained from the requirement that $\dot{w}_0 = 0$ at $t = t_f$ and the associated maximum permanent transverse displacement w_{0f} is

$$(2.11)_{1,2} \qquad \frac{w_{0f}}{H} = \frac{a_6 \nu^2 V_0^2}{2a_7 p_c H} \quad \text{or,} \quad \frac{w_{0f}}{H} = \frac{(1-\cos\phi_0)^2 \nu^2 \lambda H}{48 a_7 R},$$

where

$$(2.11)_3 \qquad\qquad \lambda = \frac{\mu V_0^2 R^2}{M_0 H}$$

is a non-dimensional impulse parameter.

Morales and Nevill [8] showed that the maximum permanent displacement field of an impulsively loaded rigid perfectly plastic continuum of density ϱ and volume V is bounded from below, viz.,

$$(2.12)_1 \qquad\qquad w_{1f\,\mathrm{max}} \geqslant \frac{t_f^c \left\{ \int \varrho V_i \dot{u}_i\, dV - \int\limits_0^{t_f^c} D(\dot{u}_i^c)\, dt \right\}}{\int \varrho \dot{u}_i\, dV},$$

where $\dot{u}_i$ is any time-independent kinematically admissible velocity field and V_i and D are defined previously,

$$(2.12)_{2,3} \qquad t_f^c = \frac{\int \varrho V_i \dot{u}_i\, dV}{D(\dot{u}_i)} \quad \text{and} \quad \dot{u}_i^c = \dot{u}_i(1-t/t_f^c).$$

If Eqs. (2.1), (2.6) and $D(\dot{u}_i) = 2\pi R^2 \dot{w}_0/(1-\cos\phi_0)$ times the right-hand side of Eq. (2.8) are substituted into (2.12), then

$$(2.13) \qquad\qquad \frac{w_{0f}}{H} \geqslant \frac{a_6 \nu^2 V_0^2}{3a_7 p_c H},$$

which is two-thirds of the value predicted by (Eq. $(2.11)_1$. The corresponding upper bound theorem of Martin [9] cannot be used in this particular case because no statically admis-

sible rigid-plastic solutions are available for a point load which acts on a deep spherical shell. A linear elastic solution is statically admissible and could be used but might not give a good upper bound.

3. Approximate dynamic response of non-symmetric shells

The analytical procedure presented in Ref. [3] can be applied, in principle, to any structure which satisfies the usual assumptions of thin-shell theory. However, a cylindrical shell panel is examined in the following section using a simple extension of the method employed by JANAS [10, 11] for the limit analysis of non-symmetric shells. In this particular procedure the structural deformation is idealized as several rigid regions separated by narrow plastic hinges. These plastic hinges are viewed mathematically as curves with certain permissible velocity discontinuities and relative rotation rates between the adjacent rigid regions and physically as narrow zones produced by severe strains and curvature changes. The total internal energy dissipation of a structure, which is concentrated in the
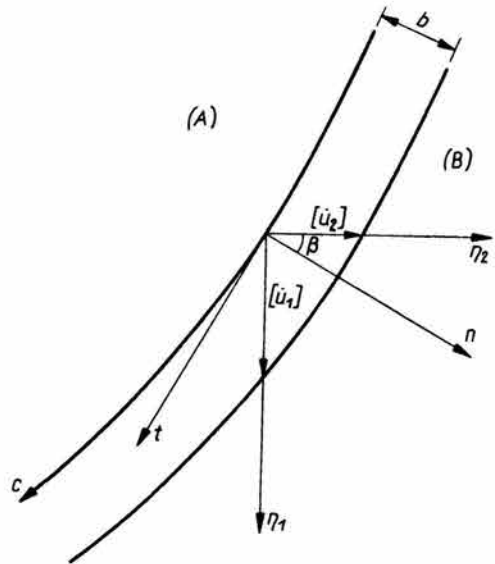

FIG. 2. Velocity discontinuities at a plastic hinge
of width b and length c.

plastic hinges, must be equal to the external work rate according to the principle of virtual work.

Consider two rigid regions A and B separated by a plastic hinge of width b as indicated in Fig. 2. If the displacement rates vary linearly across this hinge, then the strain rates are

$$(3.1)_{1-3} \quad \dot{\varepsilon}_1 = \frac{[\dot{u}_1]\sin\beta}{b}, \quad \dot{\varepsilon}_2 = \frac{[\dot{u}_2]\cos\beta}{b} \quad \text{and} \quad \dot{\gamma}_0 = \frac{[\dot{u}_1]\cos\beta + [\dot{u}_2]\sin\beta}{b}.$$

Similarly, the curvature rates are

$$(3.2)_{1-3} \quad \dot{\varkappa}_1 = \frac{\dot{\Omega}_1\sin\beta}{b}, \quad \dot{\varkappa}_2 = \frac{\dot{\Omega}_2\cos\beta}{b} \quad \text{and} \quad 2\dot{\varkappa}_{12} = \frac{\dot{\Omega}_1\cos\beta + \dot{\Omega}_2\sin\beta}{b},$$

where $\dot{\Omega}_\alpha$ are the components along the η_α axes of the relative rotation rates between the rigid regions A and B. The internal energy dissipation rate is

$$(3.3)_1 \qquad D = \int\limits_{\substack{S \\ \text{hinge}}} (N_1 \dot{\varepsilon}_1 + N_2 \dot{\varepsilon}_2 + N_{12} \dot{\gamma}_0 + M_1 \dot{\varkappa}_1 + M_2 \dot{\varkappa}_2 + 2M_{12} \dot{\varkappa}_{12}) dS$$

or, if it is assumed that the generalized stress values are uniform across a hinge zone, then

$$(3.3)_2 \qquad D = \int\limits_c \{ N_1 [\dot{u}_1] \sin\beta + N_2 [\dot{u}_2] \cos\beta + N_{12} [\dot{u}_1] \cos\beta + N_{12} [\dot{u}_2] \sin\beta$$

$$+ M_1 \dot{\Omega}_1 \sin\beta + M_2 \dot{\Omega}_2 \cos\beta + M_{12} \dot{\Omega}_1 \cos\beta + M_{12} \dot{\Omega}_2 \sin\beta \} dC,$$

since $dS = b \, dC$. The positive directions of the generalized stress resultants in Eqs. (3.3) are defined in Ref. [3].

4. Cylindrical panel

The dynamic response of the rigid, perfectly plastic cylindrical shell panel, which is illustrated in Fig. 3, is now examined using the approximate procedure outlined in the
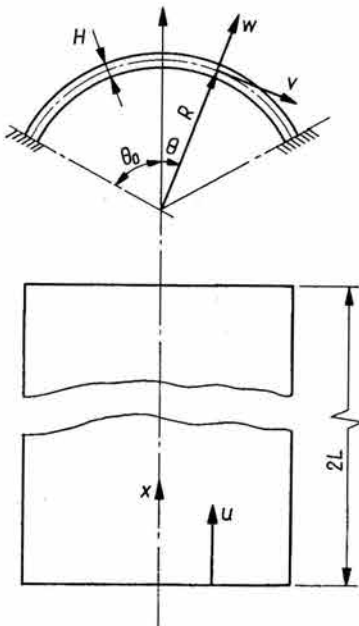

FIG. 3. Cylindrical shell panel which is fully clamped along the two longitudinal sides and free at the circumferential edges.

previous section. The panel is fully clamped along the longitudinal sides, free at the circumferential edges and is subjected to an internal impulse distributed uniformly over the zone $0 \leqslant \theta \leqslant \theta_e$. $L - l_e \leqslant x \leqslant L$ of the middle surface. This analysis is developed with the aid of the same velocity field which JANAS [10, 11] employed for the static collapse of a similar structure. Thus, in region 1 of Fig. 4

$$(4.1)_{1-3} \qquad \dot{u} = 0, \quad \dot{v} = -\dot{w}_0 \sin\theta \quad \text{and} \quad \dot{w} = \dot{w}_0 \cos\theta,$$
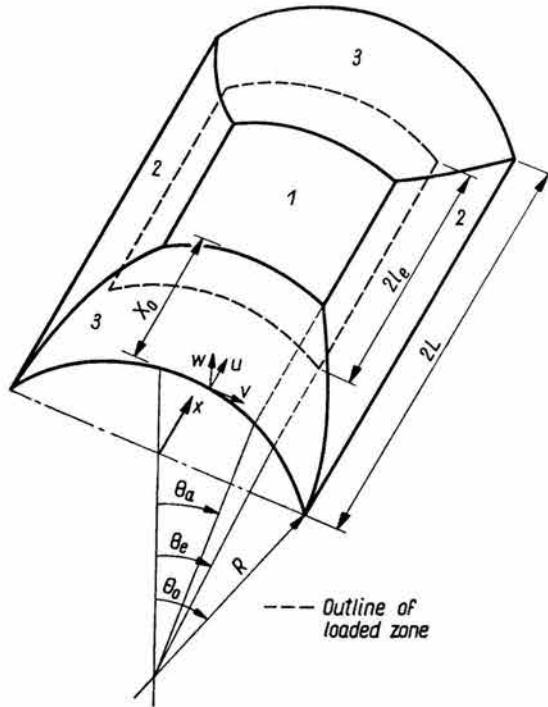
FIG. 4. Pattern of plastic hinges in a cylindrical shell panel.

in region 2

$(4.2)_{1-4}$ $\qquad \dot{u} = 0, \quad \dot{v} = \eta_a \dot{w}_0 \{1 - \cos(\theta_0 - \theta)\}, \quad \dot{w} = \eta_a \dot{w}_0 \sin(\theta_0 - \theta),$

where

$$\eta_a = \frac{\cos\theta_a}{\sin(\theta_0 - \theta_a)},$$

while in region 3

$(4.3)_{1,2}$ $\qquad \dot{u} = \dfrac{-R\dot{w}_0}{x_0}(\cos\theta - \cos\theta_0), \quad \dot{v} = \dfrac{-x}{x_0}\dot{w}_0\sin\theta$

and

$(4.3)_3$ $\qquad \dot{w} = \dfrac{x}{x_0}\dot{w}_0\cos\theta.$

Clearly w and $\dot{w}$ must be continuous throughout a panel in order to achieve zero transverse shear strains. Thus the equation for the curved plastic hinge separating regions 2 and 3 is

(4.4) $\qquad x_{23} = x_0\eta_a \dfrac{\sin(\theta_0 - \theta)}{\cos\theta}.$

The discontinuities in the various quantities at the plastic hinges according to Eqs. (4.1)–(4.3) are

$(4.5)_{1-3}$ $\qquad [\dot{u}] = 0, \quad [\dot{v}] = \{\eta_a - \eta_a\cos(\theta_0 - \theta_a) + \sin\theta_a\}\dot{w}_0, \quad [\dot{w}'] = 0,$

and

(4.5)$_4$ $$[\dot{w}^*] = \{\sin\theta_a - \eta_a\cos(\theta_0 - \theta_a)\}\dot{w}_0$$

between regions 1 and 2 $((\ )' = \partial(\ )/\partial x, \ (\ )^* = \partial(\ )/\partial\theta)$,

$$[\dot{u}] = \frac{R}{x_0}(\cos\theta - \cos\theta_0)\dot{w}_0,$$

(4.6)$_{1-3}$ $$[\dot{v}] = \eta_a\{1 - \cos(\theta_0 - \theta) + \tan\theta\sin(\theta_0 - \theta)\}\dot{w}_0,$$

$$[\dot{w}'] = \frac{-\dot{w}_0}{x_0}\cos\theta$$

and

(4.6)$_4$ $$[\dot{w}^*] = -\eta_a\{\cos(\theta_0 - \theta) - \tan\theta\sin(\theta_0 - \theta)\}\dot{w}_0$$

between regions 2 and 3,

(4.7)$_{1-3}$ $$[\dot{u}] = \frac{R}{x_0}(\cos\theta - \cos\theta_0)\dot{w}_0, \quad [\dot{v}] = 0, \quad [\dot{w}'] = \frac{-\dot{w}_0}{x_0}\cos\theta$$

and

(4.7)$_4$ $$[\dot{w}^*] = 0$$

between regions 1 and 3, and

(4.8)$_{1,2}$ $$[\dot{u}] = [\dot{v}] = [\dot{w}'] = 0 \quad \text{and} \quad [\dot{w}^*] = \eta_a\dot{w}_0$$

at the clamped boundary. It may be shown when integrating the curvature rate expressions in Ref. [3] across a plastic hinge that the relative rotation rates between conterminous rigid zones are

(4.9)$_{1,2}$ $$\dot{\Omega}_x = -[\dot{w}'] \quad \text{and} \quad \dot{\Omega}_\theta = \frac{[\dot{v}] - [\dot{w}^*]}{R}$$
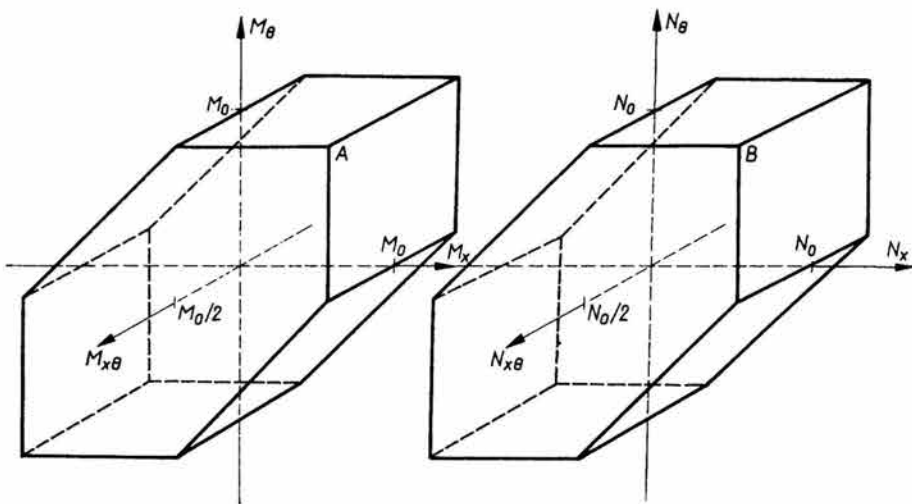

FIG. 5. Limited interaction yield surface.

The strain and curvature rates in the plastic zones may be determined by substituting Eqs. (4.5)–(4.9) into (3.1)–(3.2). Thus the normality requirements of plasticity associated with the limited interaction yield surface shown in Fig. 5 demands

$(4.10)_1$ $$M_\theta = M_0, \quad N_\theta = N_0$$

and

$(4.10)_2$ $$0 \leqslant M_x \leqslant M_0, \quad -\frac{M_0}{2} \leqslant M_{x\theta} \leqslant \frac{M_0}{2}, \quad 0 \leqslant N_x \leqslant N_0, \quad -\frac{N_0}{2} \leqslant N_{x\theta} \leqslant \frac{N_0}{2}$$

between regions 1 and 2,

$(4.11)_1$ $$M_x = M_0, \quad N_x = N_0$$

and

$(4.11)_2$ $$0 \leqslant M_\theta \leqslant M_0, \quad -\frac{M_0}{2} \leqslant M_{x\theta} \leqslant \frac{M_0}{2}, \quad 0 \leqslant N_\theta \leqslant N_0 \quad -\frac{N_0}{2} \leqslant N_{x\theta} \leqslant \frac{N_0}{2}$$

between regions 1 and 3,

$(4.12)_{1,2}$ $$M_x = M_\theta = 2M_{x\theta} = M_0 \quad \text{and} \quad N_x = N_\theta = 2N_{x\theta} = N_0.$$

between regions 2 and 3, and

$(4.13)_{1,2}$ $$M_\theta = -M_0 \quad \text{and} \quad -M_0 \leqslant M_x \leqslant 0, \quad -\frac{M_0}{2} \leqslant M_{x\theta} \leqslant \frac{M_0}{2}$$

at the clamped boundary ($\theta = \theta_0$).

Now substituting Eqs. (4.10)–(4.13) and (4.5)–(4.9) into (3.3)$_2$ gives the internal energy dissipation

$(4.14)_{1,2}$ $$D = FM_0\dot{w}_0, \quad \text{where} \quad F = F(L, R, H, x_0, \theta_a, \theta_0).$$

The external work rate for transverse loading is [3]

$(4.15)_1$ $$E = \int \left\{ (p - \mu\ddot{w})\dot{w} - \mu\ddot{u}\dot{u} - \mu\ddot{v}\dot{v} \right\} dS$$

which in view of the nature of the velocity field described by (4.1)–(4.3) may be rewritten in the form

$(4.15)_{2,3}$ $$E = (pg - \mu e\ddot{w}_0)\dot{w}_0, \quad \text{where} \quad g = g(L, x_0, l_e, \theta_0, \theta_a, \theta_e)$$

and

$(4.15)_4$ $$e = e(L, x_0, l_e, \theta_0, \theta_a).$$

Equating $(4.14)_1$ and $(4.15)_2$ provides the governing equation of motion

(4.16) $$FM_0 = pg - \mu e\ddot{w}_0.$$

The upper bound static collapse pressure $p_c^u = FM_0/g$ (from (4.16) with $\ddot{w}_0 = 0$) of a cylindrical panel of given dimensions, which is loaded within the zone $0 \leqslant \theta \leqslant \theta_e$ and $L - l_e \leqslant x \leqslant L$, is clearly a function of the mode shape parameters x_0 and θ_a. A parametric optimization was performed for discrete combinations of x_0 and θ_a and it was found over the range of parameters examined in Ref. [1] that the minimum collapse pressure occurred for $x_0 = L$ and θ_a somewhat less than θ_e. Thus region 1 in Fig. 4 degenerates into a curve as indicated in Fig. 6.
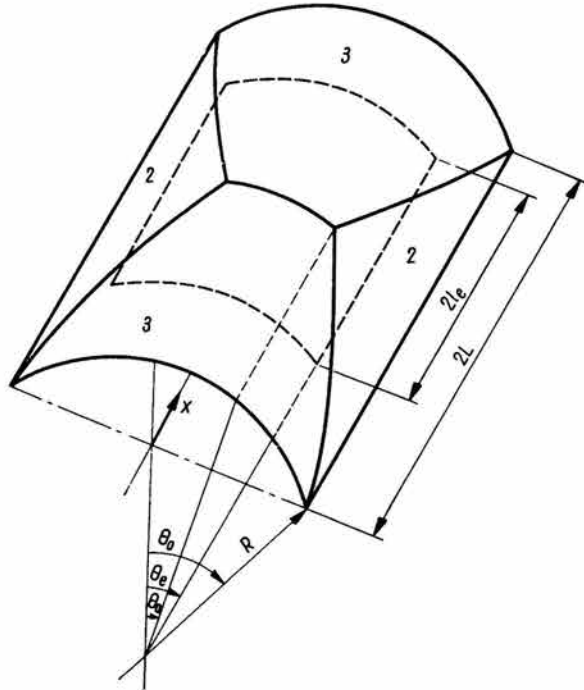
4*

Fig. 6. Optimum pattern of plastic hinges in a cylindrical shell panel.

In this case, it may be shown that

$$(4.17)_1 \quad F = \frac{4R^2}{LH}(\sin\theta_0 - \theta_0\cos\theta_0) + \frac{R}{L}\sin\theta_0 + \frac{L\eta_a}{R} + \frac{2R\eta_a}{H}\{(\theta_0 - \theta_a)$$

$$- \cos^2\theta_0(\tan\theta_0 - \tan\theta_a)\} + \frac{\eta_a}{2}\left\{(\theta_0 - \theta_a) + \cos\theta_0\ln\left(\frac{\sec\theta_0 + \tan\theta_0}{\sec\theta_a + \tan\theta_a}\right)\right\}$$

$$+ \frac{L}{R}\eta_a^2\cos\theta_0(\tan\theta_0 - \tan\theta_a) + \frac{4L}{H}\eta_a^2\cos\theta_0\left\{(\tan\theta_0 - \tan\theta_a)\right.$$

$$\left. - \frac{1}{2}\cos\theta_0\left[\ln\left(\frac{\sec\theta_0 + \tan\theta_0}{\sec\theta_a + \tan\theta_a}\right) + \tan\theta_0\sec\theta_0 - \tan\theta_a\sec\theta_a\right]\right\}$$

and

$$(4.17)_2 \quad \frac{e}{RL} = \frac{\theta_a}{3} + \frac{R^2}{L^2}\left(\frac{\theta_a}{2} + \frac{1}{4}\sin 2\theta_a - 2\cos\theta_0\sin\theta_a + \theta_a\cos^2\theta_0\right)$$

$$+ \frac{\eta_a R^2}{L^2}\left[\frac{1}{2}(\theta_0 - \theta_a)\sin\theta_0 + \frac{\sin\theta_0}{4}(\sin 2\theta_0 - 2\sin\theta_a) - \sin 2\theta_0(\sin\theta_0 - \sin\theta_a)\right.$$

$$+ (\theta_0 - \theta_a)\sin\theta_0\cos^2\theta_0 + \frac{\cos\theta_0}{4}(\cos 2\theta_0 - \cos 2\theta_a) - 2\cos^2\theta_0(\cos\theta_0 - \cos\theta_a)$$

$$\left. - \cos^3\theta_0\ln\frac{\sec\theta_0}{\sec\theta_a}\right] + 2\eta_a^2[\theta_0 - \theta_a - \sin(\theta_0 - \theta_a)] + \eta_a^3\left\{\frac{1}{3}(\theta_0 - \theta_a)\sin^3\theta_0\right.$$

$(4.17)_2$
[cont.]

$$-\sin^2\theta_0\cos\theta_0\ln\frac{\sec\theta_0}{\sec\theta_a}+\sin\theta_0\cos^2\theta_0(\tan\theta_0-\tan\theta_a-\theta_0+\theta_a)-2(\theta_0-\theta_a)\sin\theta_0$$

$$+2\cos\theta_0\ln\frac{\sec\theta_0}{\sec\theta_a}+2\sin2\theta_0(\sin\theta_0-\sin\theta_a)+2\cos2\theta_0(\cos\theta_0-\cos\theta_a)$$

$$-\sin2\theta_0\ln\frac{\sec\theta_0+\tan\theta_0}{\sec\theta_a+\tan\theta_a}-\frac{\cos^3\theta_0}{3}\left[\frac{1}{2}(\tan^2\theta_0-\tan^2\theta_a)-\ln\frac{\sec\theta_0}{\sec\theta_a}\right]\Bigg\}.$$

The MARTIN and SYMONDS mode factor [Eq. (2.5)] may be written

$(4.18)_1$
$$\nu=\frac{J}{e},$$

where

$(4.18)_2$
$$J=\frac{RL}{2}\sin\theta_a-\frac{R(L-l_e)^2}{2L}\sin\theta_e+RL\eta_a\{\sin\theta_0(\sin\theta_e-\sin\theta_a)$$

$$+\cos\theta_0(\cos\theta_e-\cos\theta_a)\}-\frac{RL\eta_a^2}{2}\Big\{\cos2\theta_0(\sin\theta_a-\sin\theta_e)$$

$$+\sin2\theta_0(\cos\theta_e-\cos\theta_a)+\cos^2\theta_0\log_e\left(\frac{\sec\theta_e+\tan\theta_e}{\sec\theta_a+\tan\theta_a}\right)\Big\}.$$

The equation of motion (4.16) for impulsive loading has the solution

(4.19)
$$w_0=\frac{-FM_0t^2}{2\mu e}+\nu V_0 t$$

when satisfying the initial conditions $w_0=0$ and $\dot{w}_0=\nu V_0$. Finally, the permanent maximum displacement is

$(4.20)_{1,2}$
$$\frac{w_{0f}}{H}=\frac{J^2\lambda}{2eFR^2},\qquad\text{where}\qquad\lambda=\frac{\mu V_0^2 R^2}{M_0 H}$$

is a non-dimensional impulse parameter.

5. Discussion

The maximum permanent transverse deflections of impulsively loaded hemispherical shells and cylindrical shell panels which are predicted by Eqs. $(2.11)_2$, (2.13) and $(4.20)_1$ are presented in Figs. 7 and 8, together with the corresponding experimental results reported in Refs. [1] and [2]. Equation $(2.11)_2$ agrees favorably with the experimental results recorded on aluminum 6061 T6 hemispherical shells with $R/H=10.9$ and $R/H=14.7$. However, the approximate procedure and the lower bound predictions of MORALES and NEVILL exhibit a greater dependence on R/H than the experimental values suggest. Equation $(4.20)_1$ was evaluated using every combination of the parameters of the aluminum 6061 T6 cylindrical shell panels which were tested in Ref. [1]. It was observed that, within plotting accuracy, all these calculations fell on the same straight line which is indicated in Fig. 8. This analysis was based on the limited interaction yield surface (Fig. 5) which circumscribes the exact Tresca yield surface. The upper straight line presented in Fig. 8
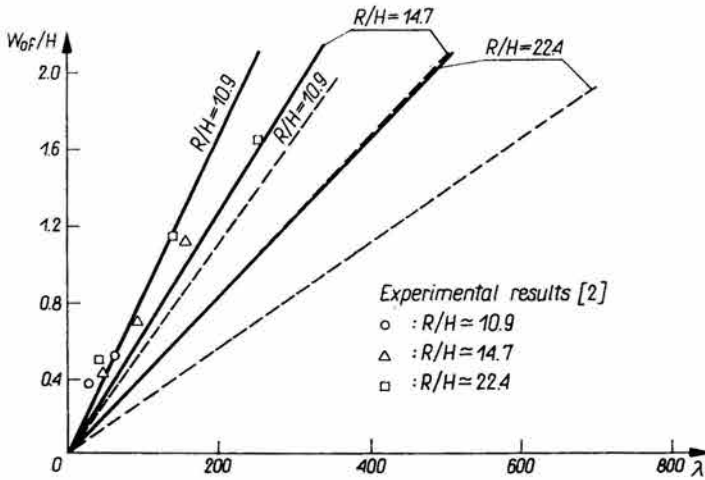
FIG. 7. Comparison of theoretical predictions and experimental results [2] on aluminum 6061T6 fully clamped deep spherical shell caps.

——————— Equation $(2.11)_2$; ———————— Lower bound of MORALES and NEVILL given by Eq. (2.13).

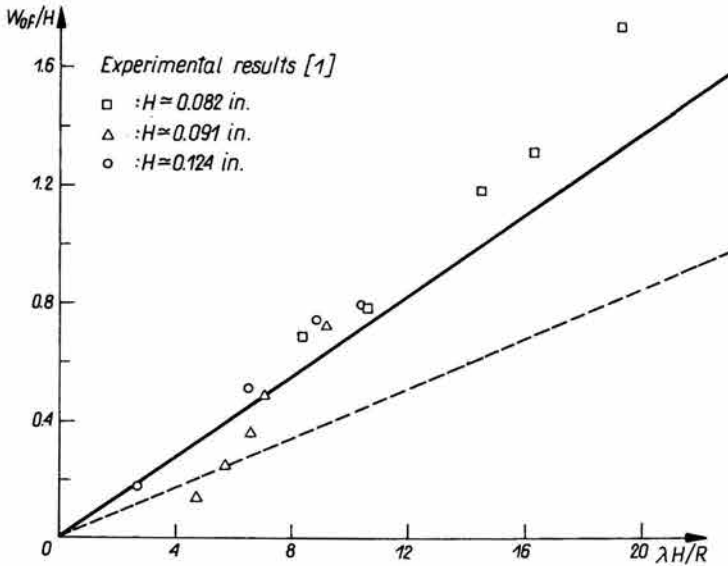
FIG. 8. Comparison of theoretical predictions and experimental results [1] on aluminum 6061T6 cylindrical shell panels.

———————— Equation $(4.20)_1$, ——————— Equation $(4.20)_1$ evaluated using $0.618 \sigma_0$.

is calculated using an approximate yield surface with a scale 0.618 times that of the circum-scribing approximate yield surface. This smaller yield surface may not completely inscribe the exact yield surface. However, no approximate yield surface which reduces to Hodge's two moment limited interaction yield surface can possibly inscribe the Tresca yield surface

with a scale factor larger than 0.618. It is not surprising that the smaller yield surface provides better agreement with the experimental results than the larger one because a large portion of the plastic hinges in this particular problem have generalized stresses corresponding to the corners A and B of the yield surface illustrated in Fig. 5. These corners lie outside the exact yield surface, while those on the smaller yield surface may lie near the exact yield surface.

The approximate theoretical results presented herein were developed for rigid perfectly plastic shells which undergo infinitesimal deflections. Thus the influence of material elasticity, strain hardening and strain rate sensitivity were disregarded. Although the comparisons between the experimental and theoretical results shown in Figs. 7 and 8 are quite encouraging, one should be mindful of the above approximations and others [3] when applying this procedure to shells with different material properties and structural geometries.

6. Conclusions

A comparison is made between the predictions of an approximate theoretical rigid-plastic procedure and some experimental values of the permanent deflections of hemispherical shells and cylindrical shell panels loaded impulsively. The initial kinetic energy of the dynamic loads in these tests was considerably larger than the maximum amount of strain energy which the shells could absorb in a wholly elastic manner. It emerged that reasonable agreement was obtained for the strain rate insensitive shells examined here and in Ref. [3] which should provide encouragement for the further development of these approximate procedures.

Acknowledgements

References

1. N. JONES, J. W. DUMAS, J. G. GIANNOTTI and K. E. GRASSIT, *The dynamic elastic behavior of shells*, Symp. Dynamic Response of Structures, Stanford 1971. To be published by Pergamon Press, Ed. G. HERRMANN.

2. N. JONES, J. G. GIANNOTTI and K. E. GRASSIT, *An experimental study into the dynamic inelastic behavior of spherical shells and shell intersections*, M.I.T., Dept. of Ocean Engineering, Report 71–15, 1971.

3. R. M. WALTERS and N. JONES, *An approximate theoretical study of the dynamic plastic behavior of shells*, M.I.T., Dept. of Ocean Engineering, Report 71–12, 1971.

4. A. SAWCZUK, *Large deflections of rigid-plastic plates*, Proc. 11th Int. Cong. App. Mech., 224–228, 1964.

5. N. JONES, *A theoretical study of the dynamic plastic behavior of beams and plates with finite deflections*, Int. J. of Solids and Structures, 7, 1007–1029, 1971.

6. E. T. ONAT and W. PRAGER, *Limit analysis of shells of revolution*, Proc. Roy. Netherlands Acad. Sci., B57, 534–548, 1954.

7. J. B. Martin and P. S. Symonds, *Mode approximations for impulsively loaded rigid-plastic structures*, Proc. A.S.C.E., **92**, EM5, 43–66, 1966.

8. W. J. Morales and G. E. Nevill, *Lower bounds on deformations of dynamically loaded rigid-plastic continua*, A.I.A.A. Journal, **8**, 11, 2043–2046, 1970.

9. J. B. Martin, *Impulsive loading theorems for rigid-plastic continua*, Proc A.S.C.E., **90**, EM5, 27–42, 1964.

10. M. Janas, *Limit analysis of non-symmetric plastic shells by a generalized yield line method*, Non-classical Shell Problems, North Holland Publishing Company, 997–1010, Amsterdam 1964.

11. W. Olszak and A. Sawczuk, *Inelastic behavior in shells*, P. Noordhoff Ltd., Groningen 1967.

MASSACHUSETTS INSTITUTE OF TECHNOLOGY
DEPARTMENT OF OCEAN ENGINEERING
CAMBRIDGE, MASS. 02139